

## Measurements of Inelastic Scattering Cross Sections for Fast Neutrons\*†

J. J. VAN LOEF‡ AND D. A. LIND

*Department of Physics, University of Wisconsin, Madison, Wisconsin*

(Received July 11, 1955)

Cross sections for inelastic neutron scattering by Fe, Mn, I, and F have been measured with a collimated neutron beam by observing the gamma radiations from the excited states. Excitation curves for the 850-keV level of Fe<sup>56</sup>, the 128-keV level of Mn<sup>55</sup> and the levels at 62, 208, 435, and 632 keV in I<sup>127</sup> were compared with the Hauser-Feshbach theory. The nuclear penetrabilities were obtained from the "cloudy crystal ball" model. In general, the best agreement with theory was obtained for the value of the nuclear absorption corresponding to a "black" nucleus. The angular distribution of the 850-keV radiation from Fe<sup>56</sup> was given by:  $W(\theta) = 1 + (0.54 \pm 0.05)P_2(\cos\theta) - (0.28 \pm 0.05)P_4(\cos\theta)$ . Excitations of levels at 980 keV in Mn<sup>55</sup>; at 390, 725, and 950 keV in I<sup>127</sup>, and at 110, 197, and 1560 keV in F<sup>19</sup> were also observed. No levels in S<sup>32</sup> or Sr below 1 Mev were found. The excitation curves cannot be used to determine spins of excited states and even where spins and parities are known the agreement with theory is not good.

### INTRODUCTION

INELASTIC scattering of neutrons offers a convenient means to study the bound energy states of medium and heavy nuclei because the uncharged neutron can readily penetrate the nuclear surface to form a compound system. Usually the decay of the system takes place with the emission of a neutron or gamma radiation. If a neutron is emitted, the target nucleus may be left in its ground state or any excited state energetically possible. By controlling the energy of the ingoing neutrons only a limited number of states will be excited. In addition, it is possible for a relatively large angular momentum transfer to take place, so that states of almost any angular momentum may be excited by the process.

Experiments on the scattering and transmission of fast neutrons by Barschall and co-workers<sup>1</sup> have resulted in a revision of earlier ideas concerning the interaction of fast neutrons with the nucleus and have given impetus to the development of the "cloudy crystal ball" model.<sup>2</sup> In the past the Bohr concept of compound nucleus formation has been used to interpret the interaction of fast neutrons with nuclei. The incoming neutron was assumed to interact strongly with nuclear matter and thus share its energy quickly; the decay of the system was independent of the mode of formation and all allowed modes of decay had the same intrinsic probability. This model, however, has not been able to account for a large number of experimental observations.

The success of the shell model suggested that the interaction of the neutron may not be strong and led to the development of the "intermediate coupling" model or the "cloudy crystal ball" model.<sup>2,3</sup> The neutron is assumed to interact with the nucleus as though it

were in a potential well. An imaginary term in the potential accounts for the formation of the compound nucleus. The potential represents the average effect of the individual levels of the compound nucleus which are usually so closely spaced that they cannot be distinguished. The potential well is given by

$$\begin{aligned} V &= -V_0(1+i\zeta), & r \leq R, \\ V &= 0, & r > R, \end{aligned} \quad (1)$$

where  $R$  is the nuclear radius,  $V_0$  is the potential depth and  $\zeta$  is the absorption parameter.  $V_0$  is usually assumed to be 42 Mev,  $\zeta$  equal to 0.05 and  $R = 1.45 \times 10^{-13} A^{1/3}$  cm. Most calculations assume a square well although calculations have been made both for a diffuse boundary<sup>4</sup> and for spheroidal-shaped wells.<sup>5</sup> If one takes appropriate averages over resonance levels, then the elastic scattering cross section may be broken into two parts.

$$\sigma_e = \sigma_{ee} + \sigma_{ce}. \quad (2)$$

$\sigma_{ee}$  is the average potential or "shape elastic" scattering cross section,  $\sigma_{ce}$  is the "compound elastic" cross section and  $\sigma_e$  is the total elastic cross section. The cross section for formation of the compound nucleus is given by the relation

$$\sigma_c = \sigma_{ce} + \sigma_r. \quad (3)$$

The reaction cross section  $\sigma_r$ , contains the inelastic scattering as well as all other possible reaction cross sections. The elastic scattering cannot be separated into the compound-elastic scattering and the shape-elastic or potential scattering, and there is no method for measuring directly the value of the cross section for compound nucleus formation. However, when only neutron scattering and capture are energetically possible, the value of the inelastic scattering cross section provides in some cases a good lower limit on the value of  $\sigma_c$ . Since this quantity is directly related to  $\zeta$ , such measurements provide a means for determining values of this parameter.

\* This work was supported by the U. S. Atomic Energy Commission and the Wisconsin Alumni Research Foundation.

† The work is discussed in detail in a thesis submitted by J. J. Van Loef to the faculty of the University of Utrecht.

‡ Now at the Physisch Laboratory, University of Utrecht, Utrecht, Holland.

<sup>1</sup> H. H. Barschall, *Am. J. Phys.* **22**, 517 (1954).

<sup>2</sup> Feshbach, Porter, and Weisskopf, *Phys. Rev.* **96**, 448 (1954).

<sup>3</sup> Lane, Thomas, and Wigner, *Phys. Rev.* **98**, 693 (1955).

<sup>4</sup> C. F. Porter (private communication) and Z. Jankovic, *Phil. Mag.* **46**, 376 (1955).

<sup>5</sup> D. C. Choudhury (communicated by L. Willets).

Inelastic scattering and compound elastic scattering are identical processes except for the different final nuclear states. The cross section for excitation of a given level will depend on the properties of the ground state and the excited state and also on the properties of the compound nucleus. Hauser and Feshbach<sup>6</sup> have calculated the cross section for inelastic scattering assuming that the statistical model is valid. In medium and heavy nuclei the level spacing in the compound nucleus at energies corresponding to the excitation energy of the system will be small compared to the level widths and to the experimental neutron energy spread. Hence many states of the compound system may be occupied and it is assumed that all possible  $J$  values and parities are found among these states. Thus in carrying out averages over resonance levels interference effects will cancel out. The resultant cross section is expressed as the product of a cross section,  $\sigma_c$ , for compound system formation and the probability that the system decays by neutron emission leaving the target nucleus in any of the states permitted by the conservation of energy and angular momentum. The cross section for compound nucleus formation,  $\sigma_c$ , is given by

$$\sigma_c = \sum_l \sigma_c^{(l)} = \sum_l (2l+1)\pi\lambda^2 T_l(E). \quad (4)$$

$\sigma_c^{(l)}$  is the partial cross section for incoming partial waves of orbital angular momentum  $l$ ;  $\lambda$  is the wavelength of the incoming neutron divided by  $2\pi$ .  $T_l(E)$  is the penetrability for  $l$  wave neutrons of energy,  $E$ , and is defined as the probability that a neutron impinging on the nuclear boundary will be captured by the nucleus. The effects of the compound nucleus properties are contained in  $T_l(E)$  and its value is given explicitly in terms of  $V_0$ ,  $\zeta$ ,  $R$ , and the neutron energy,  $E$ . It is also assumed that the breakup of the compound nucleus is governed entirely by corresponding transmission factors,  $T_{\nu'}(E')$ , where  $E'$  is the outgoing neutron energy. The final expression of Hauser and Feshbach for the cross section for excitation of a state of spin  $I'$  is

$$\sigma_{\text{in}}(I, E/I', E') = \frac{\pi\lambda^2}{2(2I+1)} \sum_l T_l(E) \times \sum_J \frac{\epsilon_{j,l}^J (2J+1) \sum_{\nu'} \epsilon_{j',\nu'}^J T_{\nu'}(E')}{\sum_{i,l''} \epsilon_{j'',l''}^J T_{\nu''}(E_{i''})}, \quad (5)$$

here  $\lambda$  is the neutron wavelength divided by  $2\pi$ ;  $I$  and  $I'$  are the spins of the ground and excited states;  $E$  and  $E'$  are the energies of the incoming and outgoing neutrons; and  $l$  and  $l'$  are the angular momenta of incoming and outgoing particles respectively.  $J$  is the spin of the compound state. Channel spins  $j$  are defined by the relations  $j_1 = I + \frac{1}{2}$  and  $j_2 = I - \frac{1}{2}$ . The sum in the denominator is over all states of the target nucleus which can be excited including the ground state and the

<sup>6</sup> W. Hauser and H. Feshbach, Phys. Rev. **87**, 366 (1952).

particular excited state with spin  $I'$  and over all outgoing partial waves,  $l''$ , which can couple with the outgoing channel spin  $j''$  to give  $J$ . The factor  $\epsilon$  is introduced to conserve angular momentum;  $\epsilon=2$  if both  $j_1 = I + \frac{1}{2}$  and  $j_2 = I - \frac{1}{2}$  satisfy the condition:  $|J-l| \leq j_i \leq (J+l)$ ;  $\epsilon=1$  if  $j_1$  or  $j_2$ , but not both, satisfies this condition; and  $\epsilon=0$  if neither  $j_1$  nor  $j_2$  satisfies the condition. Written in this manner, Eq. (5) is valid when competition between several excited states and the ground state is considered. The basic assumptions used to derive Eq. (5) are the same whether intermediate or strong coupling is valid.<sup>7,8</sup> The competition for the alternative modes of decay of the compound nucleus is given by the  $T_l(E)$  functions. The summation over  $J$  implies that all possible states formed by combination of the orbital and channel spins contribute to the scattering. There has been some evidence that a process quite analogous to Coulomb excitation exists in which the neutron excites the collective modes of the nucleus. This would be a direct interaction and exhibit different excitation and angular distribution properties. It would contribute to the absorption potential  $\zeta V_0$  but could not be expressed as a potential which is uniform over the nuclear volume.

Several investigations of inelastic scattering of neutrons have been made<sup>9</sup> in which the gamma rays from excited states were observed. To overcome the problem of low intensity a ring-shaped scatterer surrounding the detector was used, and the detector was shielded from the direct neutron beam by a suitable conical shield. The gamma-ray spectra were partially obscured because the NaI scintillation spectrometer was sensitive to scattered neutrons also. A preliminary study of the conditions about the Wisconsin electrostatic generator convinced us that the ring geometry could not be used. The results reported in this paper were obtained with a collimated beam of neutrons and a well-shielded detector. The intensity was considerably less than with the ring geometry but the background was reduced sufficiently to enable us to make adequate measurements. Furthermore much smaller samples could be used so that the troublesome corrections for multiple scattering and absorption could more easily be carried out. Finally this geometry was more suitable for angular distribution measurements.

#### EXPERIMENTAL DETAILS

The experimental arrangement is shown in Fig. 1. The collimator was of the modified Preston-Stelson

<sup>7</sup> All nuclear properties of the compound system are contained in the values of  $T_l(E)$ . Wigner *et al.*,<sup>3</sup> argue that for the low-lying excited states the values of  $V_0$  and  $\zeta$  are the same as for the ground state. It is known from experimental evidence that  $\zeta$  must be a function of energy since at 4-Mev neutron energy the interaction is much stronger than at lower energies.<sup>3</sup>

<sup>8</sup> M. Walt and J. R. Beyster, Phys. Rev. **98**, 677 (1955).

<sup>9</sup> R. B. Day, Phys. Rev. **82**, 908(A) (1953); R. M. Kiehn and C. Goodman, Phys. Rev. **95**, 989 (1954); M. J. Poole, Phil. Mag. **43**, 1060 (1952); J. M. Freeman, Phil. Mag. **46**, 12 (1955); G. L. Griffith, Phys. Rev. **98**, 579 (1955).

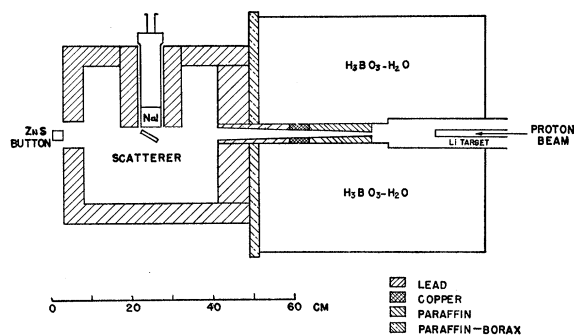


FIG. 1. Neutron scattering arrangement. A beam of neutrons from the  $\text{Li}^7(p,n)$  reaction is defined by collimating apertures placed axially in the barrel filled with  $\text{H}_3\text{BO}_3$  in water. The NaI scintillation spectrometer placed just outside the neutron beam detects the gamma radiation from the disk scatterer situated in the beam (67 cm from the neutron source). The lead shielding around the scatterer and detector is to reduce the local background radiation.

type,<sup>10</sup> and the neutrons were produced by the  $\text{Li}^7(p,n)$  reaction. The target holder projected into the axial tube through the shielding barrel which was 60 cm long by 60 cm in diameter and was filled with a saturated solution of boric acid in water. The neutron beam was collimated by paraffin and copper cylinders were placed axially in the tube so as to form a conical hole with an apex at the target. The cylindrical lead piece at the exit of the collimator served only as a gamma ray shield and did not "see" the primary neutron beam at all. The scattering chamber 30 cm on an edge was completely enclosed by 5 cm of lead save for an exit port for the primary beam. The additional shielding shown about the detector improved the background considerably. Even with no scatterer in the primary beam there was a small background flux of slow neutrons which could not be removed by extensive additional shielding. Twenty-five to 40% of the detector background was associated with neutron production.

Three detectors were used in this work. A cylindrical NaI(Tl) scintillator 4.4 cm in diameter and 5 cm in length was used for the gamma radiation, a ZnS and Lucite button was used for monitoring the neutron flux<sup>11</sup>; and a 1-cm cube of stilbene mounted on a 5 cm long Lucite light pipe was used for auxiliary neutron measurements. All the photomultipliers were connected through preamplifiers to nonoverloading amplifiers.<sup>12</sup> Either a single-channel or a 10-channel analyzer was used for pulse-height analysis. The system was linear to 1% for pulses up to 80 volts and the over-all gain was stable to about 2%.

The beam profile at the position of the scatterer is shown in Fig. 2. The detector was the stilbene crystal mounted on the Lucite light pipe. The contribution due

to gamma-ray contamination in the neutron beam is probably of the order of 1%. The observed profile agrees quite well with the geometric profile to be expected. For most of the scattering work the NaI spectrometer was set at a distance of 4.4 cm from the axis which is well outside the beam. The beam flux for  $E_n=1.2$  Mev at the scattering sample was  $1.85 \times 10^8$  neutrons/cm<sup>2</sup> microcoulomb.

The energy spread of the neutron beam from the lithium target was about 80 keV as determined by the threshold rise. To determine the true energy spectrum emerging from the collimator, a transmission experiment was performed in the region of the 445-keV neutron resonance in O<sup>16</sup>. This resonance has been carefully measured at high resolution.<sup>13</sup> The neutron transmission of a stannic oxide ( $\text{SnO}_2$ ) scattering sample was determined as a function of neutron energy.  $\text{SnO}_2$  was packed into a thin-walled iron can 3 cm in diameter. The 1-cm cubic stilbene detector was located 14 cm behind the scattering sample and was biased to detect primarily neutrons but some 478-keV gamma rays from the beta decay of  $\text{Be}^7$  in the Li target were also detected. The experimental transmission curve shown as the solid line in Fig. 3 has been corrected for transmission of the iron can and for the small gamma-ray contamination in the neutron beam. The transmission function was calculated using the total cross section data for Sn and

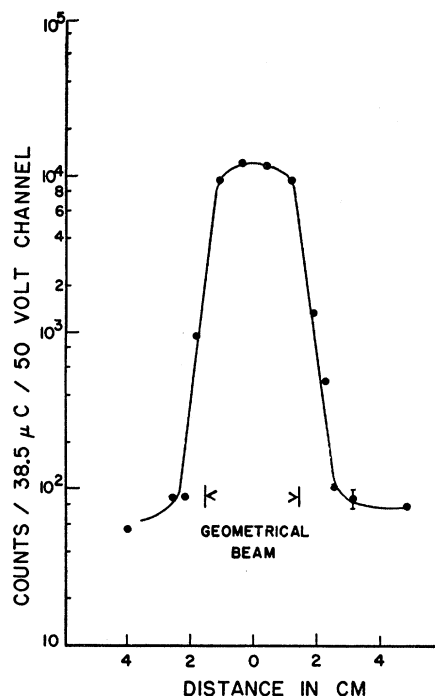


FIG. 2. Profile of the collimated neutron beam. The neutron beam profile at the position of the scattering sample was measured with a stilbene detector 1 cm on an edge biased to count neutrons. The distances are measured from the collimator axis and the vertical bars indicate the geometrical limits of the beam defined by the collimator.

<sup>10</sup> P. H. Stelson and W. M. Preston, Phys. Rev. **86**, 132 (1952).

<sup>11</sup> This button was kindly supplied by Dr. W. Hornyak of the Brookhaven National Laboratory.

<sup>12</sup> We are indebted to Mr. C. Johnstone of the Los Alamos Scientific Laboratory for supplying us with the design of the Model 250 amplifier.

<sup>13</sup> R. L. Becker (private communication).

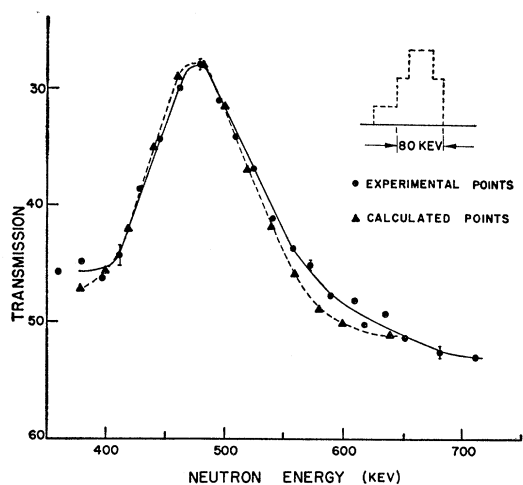


FIG. 3. The 435-kev resonance peak in the total neutron cross section of  $O^{16}$ . The circles represent the transmissions measured with a stilbene detector through an  $SnO_2$  scattering sample. The resonance width is 45 keV. The dashed curve is the transmission calculated from the true resonance curve and the assumed energy spectrum shown in the insert. The match is sensitive to the magnitude of the low-energy tail, which was set at 15%, but not to its shape.

$O^{16}$  assuming the energy distribution to be that given by the histogram shown in the inset. The dashed curve represents this function. The fit is the best that could be attained and is quite sensitive to the amount but not to the shape of the low-energy tail on the neutron distribution. The tail amounts to about 15% of the total intensity; this result is in qualitative agreement with measurements by Rosen<sup>14</sup> using photographic plates. A histogram of the form shown in Fig. 3 was used to analyze the scattering data. Fortunately a precise knowledge of the neutron energy distribution is not necessary for our measurements.

The scattering samples were in the form of disks 43 mm in diameter and about 10 mm thick. When necessary the samples in powder form were pressed into thin walled aluminum cans. The sample was located accurately with respect to the primary beam and detector and oriented so its normal made an angle of  $60^\circ$  with the beam direction. In addition, the sample could be dropped out of the beam. The supporting assembly and aluminum can contribute no background.

The neutron flux was monitored by a ZnS-Lucite button which in turn was calibrated by comparison with a standard long counter. The ZnS button was operated at a bias such that  $Co^{60}$  gamma rays were counted with an intrinsic efficiency of 0.001%. The efficiency for neutrons as a function of energy is given in Fig. 4; the efficiency represents the fraction of those neutrons incident on the detector which produce output pulses greater than the bias setting. Below 500-kev neutron energy, the long counter was used as a monitor. In all experiments, the monitor detector was

<sup>14</sup> L. Rosen, Los Alamos Scientific Laboratory (private communication).

placed behind the scattering sample and outside the lead house. Since readings were taken with the sample in and out of the beam, the monitor data gave the average transmission of the sample for neutrons. This value was usually about 20%.

The absolute calibration of the neutron flux was made by comparing with a long counter the yield of 1-Mev neutrons from the  $Li^{7}(p,n)$  source with that of a calibrated Ra-Be neutron source.<sup>15</sup> The long counter was built according to the recipe of Hanson and McKibben,<sup>16</sup> and the sensitivity was assumed to be independent of energy. Yields at other neutron energies were based on the long-counter response. The accuracy of the flux calibration was estimated to be 12%; this includes the 7% uncertainty in the primary standard.

The cross section for capture of neutrons by  $I^{127}$  has been measured with an accuracy of 7%.<sup>17</sup> The error in this measurement results almost entirely from the error in the primary neutron standard. A NaI scintillation crystal of known weight and size was bombarded for a given time in the neutron beam and then placed on a photomultiplier. The absolute beta activity was measured at zero bias as a function of time after it was ascertained that only the 25-min  $I^{128}$  activity was present. Several determinations of the neutron flux obtained by this method were consistently 15% lower than the value obtained by comparison with the standard Ra-Be neutron source so were not used except as a rough check.

The NaI detector was calibrated by using a set of standard gamma-ray sources made up as disks the same diameter as the scattering samples. Sources of  $Ce^{144}$ ,  $Hg^{203}$ , and  $Na^{22}$  gave calibration lines at 0.080, 0.134, 0.279, 0.511, and 1.28 Mev. The strength of the

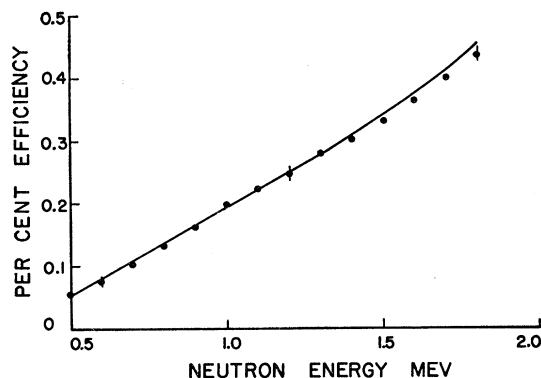


FIG. 4. The absolute efficiency of the ZnS-Lucite button used as a flux monitor. The efficiency was determined as a function of neutron energy by comparing the response with that of a long counter. The bias was set so that  $Co^{60}$  gamma radiation (1.25 Mev) was detected with an efficiency of 0.001%. The solid curve represents the value when a correction is made for the second group of neutrons from the  $Li^{7}(p,n)Be^7$  reaction.

<sup>15</sup> We are indebted to Dr. C. Eggler of the Argonne National Laboratory for calibrating our Ra-Be source against the Argonne standard neutron source.

<sup>16</sup> A. O. Hanson and J. L. McKibben, Phys. Rev. **72**, 673 (1947).

<sup>17</sup> H. C. Martin and R. F. Taschek, Phys. Rev. **89**, 1302 (1953).

Na<sup>22</sup> source was determined by comparison with Co<sup>60</sup> sources standardized at the National Bureau of Standards. The other sources were calibrated by passing a narrow collimated gamma-ray beam through a NaI crystal 5 cm long. The transmission of the crystal for the gamma radiation was always less than 10%. The complete pulse-height spectrum and the solid angle subtended at the source by the collimation diaphragm were sufficient to determine the absolute gamma-ray yield of the sources. Absolute efficiency and energy calibrations of the NaI detector were then made by placing the disk sources at the position of the center plane of the scattering samples. Figure 5 shows the counting efficiency of the system as a function of gamma-ray energy when the area under the photopeak only is used. The bars on the points indicate the probable deviations due to counting statistics alone.

During the neutron scattering experiment the complete pulse-height spectra with and without scatterer

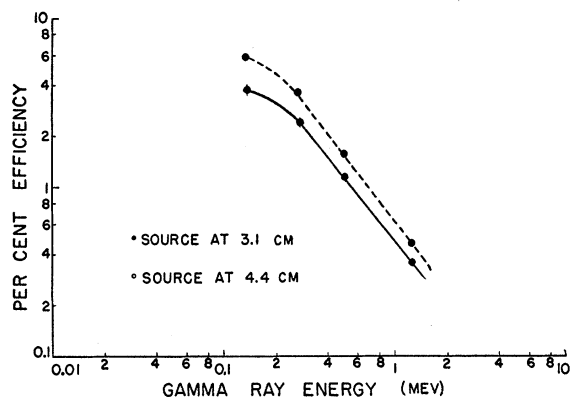


FIG. 5. The absolute efficiency of the NaI detector as determined by the number of pulses in the photopeak per photon emitted by the source plotted against gamma-ray energy. The crystal was 4.4 cm in diameter and 5 cm thick. The sources were disks 4 cm in diameter placed at the same position as the scattering sample. The distance was measured from the face of the crystal to the center of the source.

and with a carbon scatterer<sup>18</sup> were taken. The angular distribution of the elastically scattered neutrons from the sample<sup>19</sup> and from carbon<sup>20</sup> are known so that corrections for the effect of neutrons scattered into the detector crystal could be made. These corrections were important only for measurements under 500 keV.

The corrections for gamma-ray attenuation, neutron self-absorption, and multiple scattering in the sample are the most difficult to make. Fortunately the use of small scattering samples usually made these corrections small. The attenuation of the neutron beam by most samples was less than 30%; however, the correction for

<sup>18</sup> A carbon scatterer of approximately the same attenuation for neutrons as the scattering sample gives a good indication of the effect of neutrons on the detector crystal since no inelastic neutron scattering can occur below 4.35 MeV, the energy of the first excited state of C<sup>12</sup>.

<sup>19</sup> M. Walt and H. H. Barschall, Phys. Rev. **93**, 1062 (1954).

<sup>20</sup> Willard, Blair, and Kington, Phys. Rev. **98**, 669 (1955).

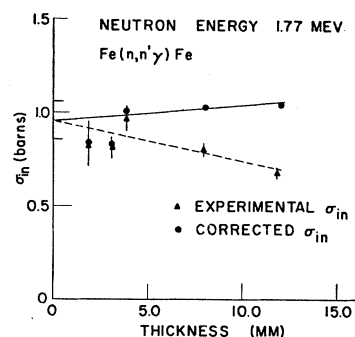


FIG. 6. The observed cross section for the reaction  $\text{Fe}^{56}(n, n')\text{Fe}^{56}$  (850-keV gamma ray) plotted versus the sample thickness for 1.77-MeV neutrons. The dashed curve is fitted to the observed data, and the horizontal bars on the ordinate axis indicate the probable error of the true cross section. The solid points are the values corrected for neutron and gamma-ray attenuation in the sample. The negative slope of the solid curve probably results from multiple scattering in the sample.

the attenuation of the low-energy gamma rays was 60 to 70%. A correction factor which gave the ratio of the observed yield to the true yield was calculated for each sample. The sample was divided into a number of thin circular disks and the true neutron flux incident on each slab was computed. The counting efficiency for gamma radiation from the slab could also be computed since the efficiency for a distributed disk source of the same geometry was known. The summation over all slabs yielded a factor,  $F$ , which related the true inelastic cross section to the observed cross section. This relation is given by  $\sigma_o = F\sigma_T$ .  $\sigma_o$  is the experimental cross section calculated from the observed neutron flux incident on the sample and  $\sigma_T$  is the true cross section. For an 8-mm thick iron disk the value of  $F$  is 0.80 for the 850-keV gamma ray and 0.50 for the 128-keV line of Mn<sup>55</sup>. An

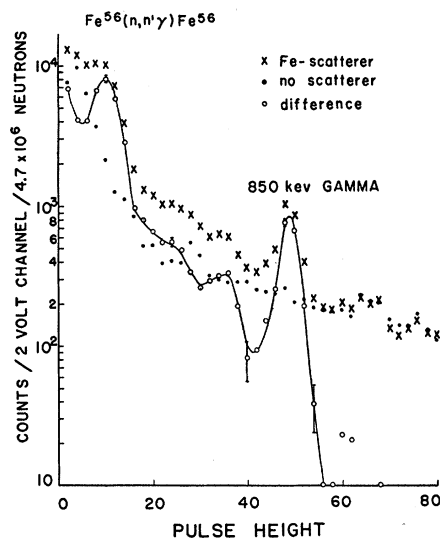


FIG. 7. Pulse-height spectrum for the gamma radiation observed from Fe<sup>56</sup> at a neutron energy of 1.2 MeV. The crosses and dots are the spectra obtained with and without the Fe scatterer respectively. The open circles represent the difference spectrum.

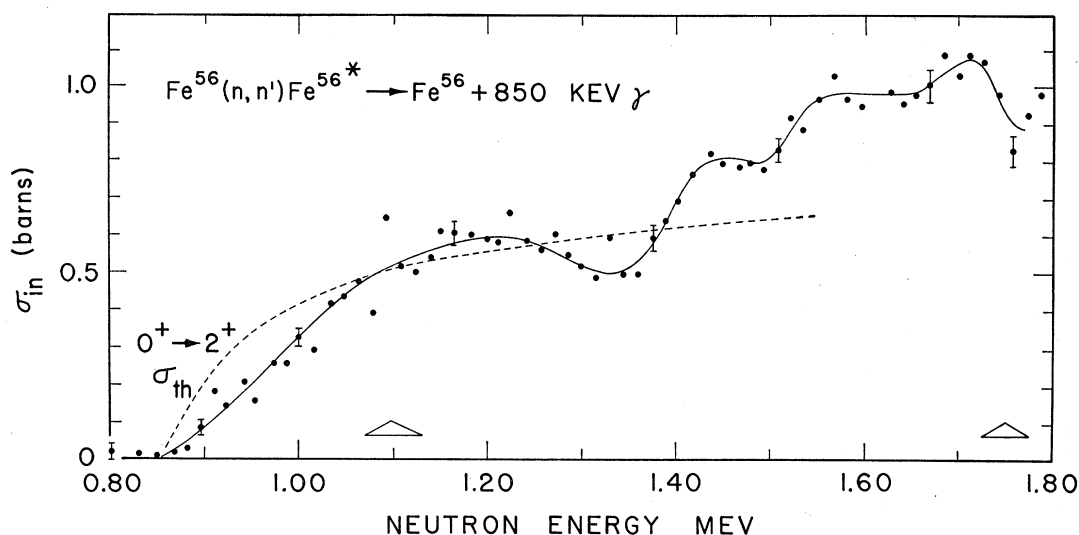


FIG. 8. Excitation curve for the 850-keV gamma ray following inelastic scattering of neutrons by  $\text{Fe}^{56}$ . The neutron energy spread, indicated by the width of the triangles, is sufficiently broad to give a partial average over residual resonance effects. The full curve was drawn to represent the mean value of the cross section as a function of energy. The points which deviate considerably indicate resonance effects. The dotted curve is calculated from the Hauser Feshbach theory for an opaque nucleus with the spin assignments shown.

estimate of the multiple scattering in the Fe sample shows that 10% of the incident neutrons suffer multiple scattering in the disk. An experimental check of the corrections discussed above was made for iron. Figure 6 shows the experimental cross section plotted as a function of sample thickness. All samples were 43 mm in diameter and were placed with their planes making an angle of 30 degrees with the beam direction. The dashed curve represents the best fit to the experimental values; the value obtained by extrapolation to zero thickness should be the true observed cross section. The horizontal bars on the ordinate axis indicate the limits of error of the extrapolated cross section. When corrections for all effects except multiple scattering are made, one obtains the solid curve. The slight downward slope toward zero sample thickness represents the effect of multiple scattering and agrees with the estimate made above.

## RESULTS AND DISCUSSION

### Iron

The reaction  $\text{Fe}^{56}(n, n')\text{Fe}^{56*}$  has been studied extensively.<sup>21</sup> States are known at 0.85, 2.04, and 2.25 Mev from studies made with neutron energies up to 2.8 Mev. In the work of Keihn and Goodman the energy resolution was sufficient to show the resonance structure, whereas in our work the effects of resonances are partially averaged out. Figure 7 shows the pulse-height spectrum of the 850-keV gamma ray obtained with and without an iron scatterer. The difference spectrum is the sum of the true gamma ray and the neutron effects

in the detector crystal. Above the 850-keV photopeak the difference spectrum dropped almost to zero, so an excitation curve was taken by observing the difference between a single channel set to bracket the photopeak and an equal channel set just on the high-energy side of the peak. Figure 8 shows the excitation curve obtained in this way. The triangles indicate the extent of the energy spread of the neutron beam. The points show some residual effects of the numerous resonances seen with higher resolution,<sup>21</sup> however, for the purpose of testing the Hauser-Feshbach theory we have drawn the full line so as to average over the resonance effects. The theoretical curve calculated for the complex square potential well given by  $V = V_0(1 + i\zeta)$  with parameters  $V_0 = 42$  Mev,  $\zeta = 0.2$ , and  $R = 1.45 \times 10^{-13} A^{1/2}$  is shown.<sup>22</sup> No spin-orbit interaction was used.

Several independent measurements of the inelastic scattering cross section were made at  $E_n = 1.18$  Mev. The value obtained for  $\sigma_{in}$  was  $0.56 \pm 0.08$  barn after corrections for the neutron and gamma-ray attenuation as well as for multiple scattering had been applied. A correction of 15% has also been applied for the angular distribution anisotropy. The accuracy of the result is limited mainly by an estimated 12% uncertainty in the absolute neutron flux calibration and an estimated uncertainty of 5% in the gamma-ray detection efficiency. The other sources of error are insignificant in comparison. When the value at  $E_n = 1.0$  Mev is corrected for the energy spread in the neutron beam, one obtains a value of  $0.39 \pm 0.04$  barn. Beyster *et al.*<sup>23</sup> report a

<sup>21</sup> R. M. Keihn and C. Goodman, Phys. Rev. **95**, 989 (1954); G. L. Griffith, Phys. Rev. **98**, 519 (1955); Jennings, Weddell, Alexeff, and Hellens, Phys. Rev. **98**, 582 (1955).

<sup>22</sup> We are indebted to Dr. R. G. Thomas of the Los Alamos Scientific Laboratory for running the computations of all  $T$  values used in these calculations.

<sup>23</sup> Beyster, Henkel, and Nobles, Phys. Rev. **97**, 563 (1955).

value of  $0.41 \pm 0.04$  barn for the nonelastic cross section obtained from sphere measurements at this energy.

In order to check the Hauser-Feshbach relation [Eq. (5)], the excitation curve in the vicinity of the threshold was plotted after the effect of the neutron energy spread was removed. Figure 9 shows this curve as a solid line up to  $E_n = 1.25$  Mev. The point at 1.18 Mev is the best value of the cross section obtained from our measurements, and the point at 1.0 Mev is the value obtained by Beyster *et al.*<sup>23</sup> For purposes of comparison with theory, partial waves up to  $l=3$  were assumed to be present in the incoming beam. Spin and parity assignments of  $0+$  and  $2+$  were made for the ground and excited states, respectively. Other spin assignments are excluded by the systematics of even-even nuclei and the angular distribution data, although  $J=1$  for the excited state cannot be ruled out by the excitation data. Values of the transmission coefficients,  $T_l$ , calculated for  $\zeta=0.04$  and  $0.2$  were used in Eq. (5) for  $\sigma_{in}$ . The dashed curve of Fig. 9 shows the result for  $\zeta=0.2$  and the dash-dot curve that for  $\zeta=0.04$ . The agreement between the curve for  $\zeta=0.2$  and experiment is perhaps fortuitous but indicates that  $\zeta=0.04$  does not give a sufficiently large cross section.

The angular distribution of the 850-keV gamma ray was measured at  $E_n = 1.77$  Mev. For these measurements the detector crystal, 4.4 cm in diameter by 5 cm long, was suspended vertically so that the center line was 7.5 cm from a cylindrical scatterer 2 cm in diameter by 4 cm long. The detector was mounted on a lead plate which enclosed the top of the house constituting the scattering chamber. The assembly of detector and plate

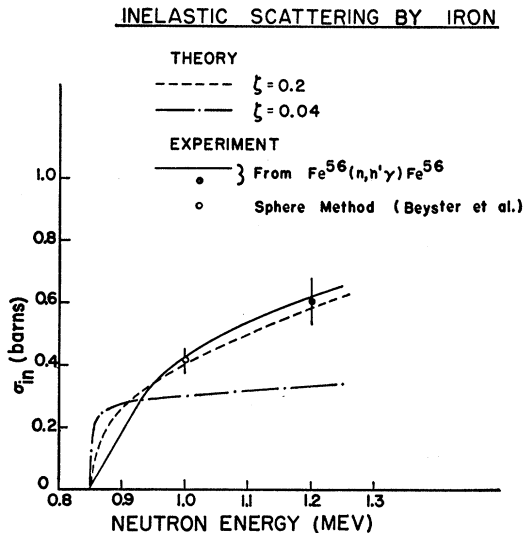


FIG. 9. Comparison of the experimental and theoretical cross sections near the threshold for the 850-keV line of  $Fe^{56}$ . The full curve represents the experimental cross section. The value is 1.2 Mev of  $0.56 \pm 0.08b$  is the best determination of the cross section from this work; the point at 1.0 Mev of  $0.41 \pm 0.04b$  is the value given by Beyster *et al.*,<sup>23</sup> for the natural element. The two theoretical curves are calculated from the Hauser-Feshbach theory for  $\zeta=0.04$  and  $0.2$ .

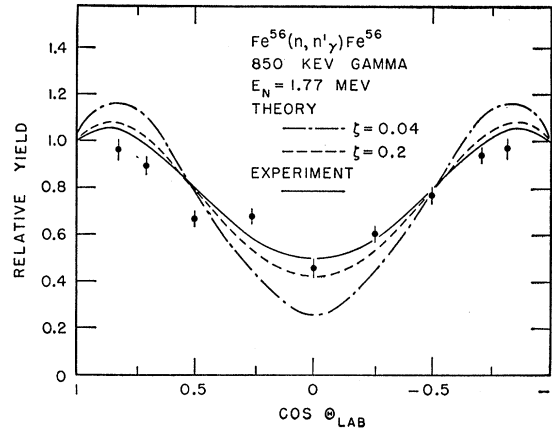


FIG. 10. The angular distribution of the 850-keV gamma radiation excited by the  $Fe^{56}(n,n')Fe^{56}$  reaction at 1.77-Mev neutron energy. The full curve represents a least-squares fit to the experimental points which have been corrected for the finite aperture of the detector and size of the source. It is given by the expression  $W(\theta) = 1 + (0.54 \pm 0.05)P_2 - (0.28 \pm 0.05)P_4$ . The dashed curves are distributions calculated from the Hauser-Feshbach theory for values of  $\zeta=0.04$  and  $0.2$  with spin assignments of  $0+$  and  $2+$  for the ground and first excited state, respectively.

could be rotated through 360 degrees so that observations on both sides of the neutron beam could be made between angles of  $25^\circ$  and  $160^\circ$ . The yield was taken as the difference between a channel bracketing the photopeak and an equal channel at the high-energy side of the line. Preliminary checks with a carbon scatterer indicated that neutron effects were entirely negligible. Figure 10 shows the experimental points which represent the average of values taken on both sides of the neutron beam. The full curve represents a least-squares fit to the experimental points. Corrections have been applied for the angular resolution of the detector and the size of the scatterer by the method of Feingold and Frankel.<sup>24</sup> The experimental distribution function is given by the expression  $W(\theta) = 1 + (0.54 \pm 0.05)P_2(\cos\theta) - (0.28 \pm 0.05) \times P_4(\cos\theta)$ . Satchler<sup>25</sup> has calculated the triple correlation function for inelastically scattered neutrons and gamma rays on the assumption of a statistical model as used by Hauser and Feshbach.<sup>6</sup> If one integrates Satchler's expression over angles of the outgoing neutrons, one obtains the relation:

$$W(\theta) = 2T_0(E)T_2(\bar{E}) + T_1(E)T_1(\bar{E})[5 + P_2(\cos\theta)] \\ + T_2(E)T_0(\bar{E})[2 + 2.713P_2(\cos\theta) \\ - 1.716P_4(\cos\theta)], \quad (6)$$

where  $\theta$  is the angle of observation of the radiation with respect to the neutron beam;  $E$  and  $\bar{E}$  ( $\bar{E} = E - 850$  keV) are the ingoing and outgoing neutron energies, respectively. Partial waves for  $l \leq 2$  are considered and the level assignment of  $0+$  and  $2+$  for the ground and first excited states respectively is made. If Eq. (6) is written as  $W(\theta) = 1 + a_2P_2(\theta) + a_4P_4(\theta)$ , the values of

<sup>24</sup> A. M. Feingold and S. Frankel, Phys. Rev. **97**, 1025 (1955).

<sup>25</sup> G. R. Satchler, Phys. Rev. **94**, 1304 (1954).

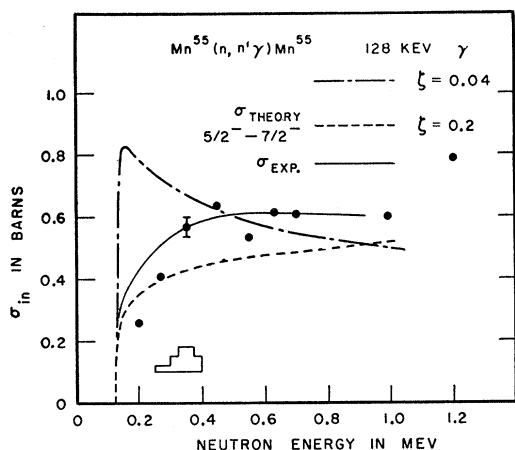


FIG. 11. Excitation curve for the 128-Mev gamma ray from  $Mn^{55}$ . The experimental curve has been corrected for the neutron energy spectrum shown by the histogram. The theoretical curves were calculated for values of  $\zeta=0.04$  and  $0.2$  assuming that the excited state has spin  $7/2$ . The high point at  $1.2$  Mev is probably real and represents the effect of a cascade transition from the  $0.98$ -Mev level.

$a_2$  and  $a_4$  are  $0.893$  and  $-0.554$  respectively for  $\zeta=0.04$  and  $0.651$  and  $-0.360$  for  $\zeta=0.2$ . The dash curve in Fig. 10 is the value for  $\zeta=0.2$ ; the dot-dash curve that for  $\zeta=0.04$ . Experimental effects such as multiple scattering in the scatterer and spurious background tend to decrease the anisotropy. Again  $\zeta=0.2$  seems to give the best agreement with experiment. There is little error introduced by the restriction to partial waves with  $l \leq 2$ .

### Manganese

A state at  $128$  kev is well known in  $Mn^{55}$  from Coulomb excitation studies.<sup>26</sup> In addition, a state at  $0.98$  Mev has been observed in the  $(n,n')$  reaction by Freeman<sup>27</sup> who reports that  $95\%$  of the decays of the  $0.98$ -Mev state go to the  $128$ -kev state and  $5\%$  to the ground state. The excitation function was measured from  $200$  kev to  $1.2$  Mev by using a powdered manganese target. The results are shown in Fig. 11. The full curve represents the best fit to the experimental points after correction for the energy spread of the neutron beam is made. The histogram is the assumed neutron energy spectrum. At  $E_n=650$  kev, the cross section,  $\sigma_{in}$ , for excitation of the  $128$ -kev level is  $0.59 \pm 0.10$  barn.<sup>28,29</sup> The point at  $1.2$  Mev is quite high although there is

<sup>26</sup> G. M. Temmer and N. Heydenburg, Phys. Rev. **96**, 426 (1954).

<sup>27</sup> J. M. Freeman, Phil. Mag. **46**, 12 (1955).

<sup>28</sup> No correction for the internal conversion of the radiation is made. The Coulomb excitation work indicates that only  $E2$  or  $M1$  transitions are possible, hence the correction would not be larger than about  $10\%$ . Guernsey<sup>29</sup> has obtained an excitation curve for the  $128$ -kev line by a different technique which employs a very thin crystal and scatterer. The combination is placed directly in front of the neutron source together with a lead filter to remove gamma radiation from the source. The values for  $\sigma_{in}$  which she obtains are about one-half those given in Fig. 11.

<sup>29</sup> J. Guernsey, Massachusetts Institute of Technology Progress Report, Feb. 28, 1955 (unpublished).

considerable spread in the points. When the level is  $0.98$  Mev was reported,<sup>27</sup> we re-examined our pulse height data and concluded that a line at  $0.84 \pm 0.04$  Mev was present and that the cross section for excitation was  $0.15 \pm 0.06$  barn at  $E_n=1.2$  Mev. This is to be compared with the value of  $0.21 \pm 0.08$  barn obtained by Freeman. The excitation curves were calculated from Eq. (5) assuming the  $128$ -kev level to be a  $7/2$ -state. If the ground state assignment of  $5/2$ -<sup>30</sup> results from the coupling of a  $(f_{7/2})^{-3}$  proton configuration, one should also expect a low-lying  $7/2$ - state and Coulomb excitation studies<sup>26</sup> do not rule out the  $7/2$ - assignment. All other assignments gave a lower cross section but the experimental data cannot be used

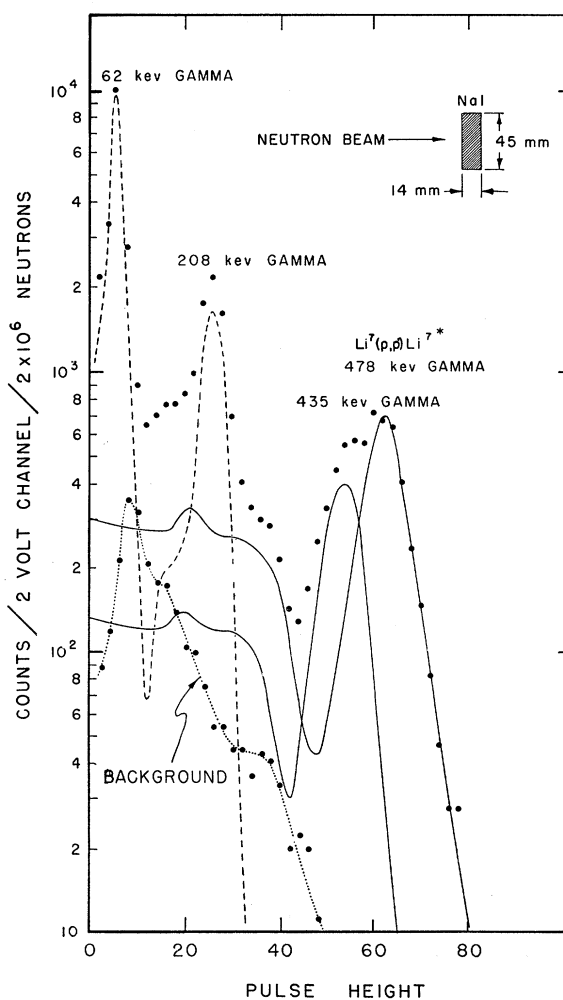


FIG. 12. Pulse-height spectrum produced by  $640$ -kev neutrons falling on a NaI scintillation crystal. The open circles represent the gross spectrum which includes gamma radiation from the neutron source as well. No  $440$ -kev gamma radiation from the first excited state of  $Be^7$  is present at this energy. The decomposition into the  $478$ -kev radiation from  $Li^7$ , and peaks at  $435$ ,  $208$ , and  $62$ -kev from  $I^{127}$  is shown. The dashed curve represents the net spectrum when the effects of the higher energy lines and background are removed.

<sup>30</sup> P. F. A. Klinkenberg, Revs. Modern Phys. **24**, 63 (1952).



determine the spin because the theory of the process is not sufficiently reliable. The dash curve represents the value for  $\zeta=0.2$  and the dot-dash curve that for  $\zeta=0.04$ . The large peak at the threshold is the result of an  $S$  wave giant resonance for low neutron energy in this mass region.<sup>31</sup>

### Iodine

Early in the investigation it became evident that the NaI detector crystal showed spurious peaks arising from neutron bombardment. There is also evidence that peaks belonging to  $I^{127}$  have been reported in the literature as gamma rays from other scatterers under investigation. A sample of crystalline iodine was packed into a standard aluminum container; the sample thickness was such that the  $F$  factor which corrects for neutron attenuation and gamma-ray self-absorption was approximately 0.8 for the 435-kev line. The contribution to the line intensity from neutron in-scattering to the NaI detector was determined by using a carbon scatterer to be about 25%. Corrections for this effect were applied to all the data obtained with the external iodine scatterer. Because of the strong self-absorption for gamma rays in the sample, the peaks below 400 kev result almost entirely from neutron scattering. The yield of the 62- and 208-kev lines were obtained by bombarding a NaI crystal mounted on a photomultiplier with the primary neutron beam. Figure 12 shows the pulse height spectrum produced by 640-kev neutrons. The gross spectrum includes the 478-kev gamma radiation from that state in  $Li^7$  but no 440-kev gamma ray from the first excited state of  $Be^7$  was present at this neutron energy. The decomposition into the 478-kev line and lines at 435, 208 and 62 kev from  $I^{127}$  is shown. The pulse-height distributions obtained for standard sources placed on the NaI crystal were used to determine the line profile for a single gamma ray. In the analysis of the data corrections had to be made for the

TABLE I. Summary of data from inelastic scattering of neutrons by  $I^{127}$ .

Observed gamma-ray energies (kev)		Beta decay of $Xe^{127}$ b	Inelastic scattering cross section (barns) c	Neutron energy (Mev)
This work	Day <sup>a</sup>			
31±2				
62±2	58	57	0.30±0.05	0.40
145±5	138	145		
		170		
208±2	204	200	0.31±0.08	0.65
390±10	396	365		
435±4	441		0.44±0.12	1.18
632±6	634		0.59±0.10	1.18
750±20	742			
950±20				

<sup>a</sup> See reference 32.

<sup>b</sup> See reference 34.

<sup>c</sup> An isotropic angular distribution is assumed for the radiation.

<sup>31</sup> The effects of the resonance are not seen in the case of  $Fe^{56}$  because the excitation energy of 850 kev brings one out of the energy range where the resonance effects are greatest.

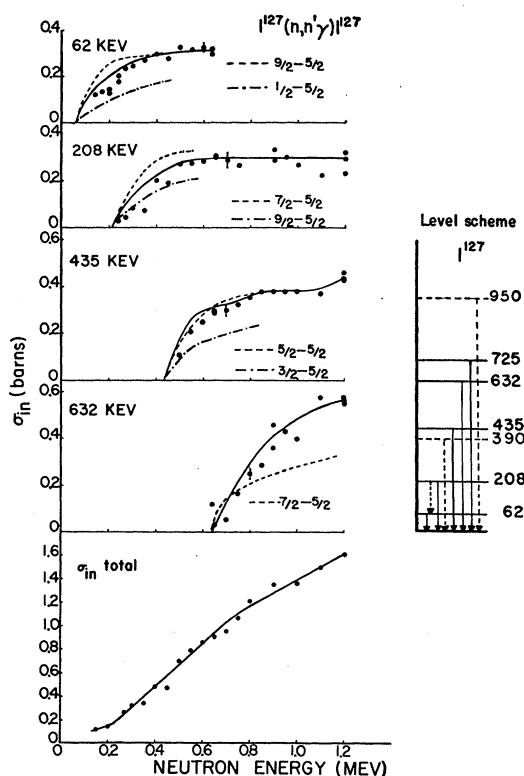


Fig. 13. The experimental excitation curves for the 62-, 208-, 435- and 632-kev radiations from  $I^{127}$  excited by the  $(n,n'\gamma)$  reaction. The full curves are experimental curves corrected, however, for the energy spread of the neutron beam.  $\sigma_{in}(\text{total})$  represents the sum of the cross sections obtained for the four lines. The 62-kev cross section is assumed to remain constant at 0.30 barn, but no contribution of the 390- or 725-kev levels is included. The dotted transitions in the level scheme are weak compared to the full lines, and no other cascade transitions were observed. See text for the discussion of the excitation curves.

escape of radiation and for the ratio of the photopeak to the total number of pulses in the differential pulse height spectrum. No corrections were made for neutrons scattered into the crystal by the surrounding material, but that effect should have been less than 10%.

The results on the excitation of  $I^{127}$  are summarized in Table I and in Fig. 13. The gamma rays are listed in Table I along with values reported by Day<sup>32</sup> for neutron excitation.<sup>33</sup> From beta-decay studies of  $Xe^{127}$ , there is evidence of levels at 58, 200, and 365 kev.<sup>34</sup> Figure 13 shows the excitation curves obtained for the 62-, 208-, 435-, and 632-kev lines, and a proposed level scheme based on these observations. The data have not been corrected for internal conversion; the 62- and 208-kev lines need no such correction. The full curve in each case is the excitation curve corrected for the spread in

<sup>32</sup> R. B. Day, Los Alamos Scientific Laboratory (private communication).

<sup>33</sup> Coulomb excitation studies by R. H. Davis and A. Divatia in this laboratory have shown the existence of the same levels reported in Table I.

<sup>34</sup> I. Bergstrom, Arkiv Fysik 5, 191 (1952); H. Mathur, Phys. Rev. 97, 707 (1955).

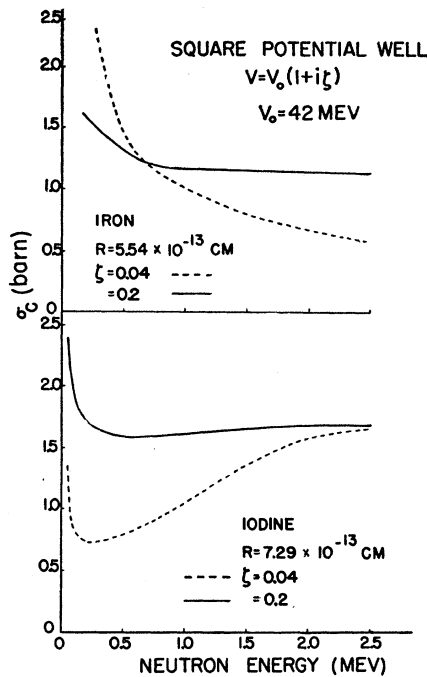


FIG. 14. Theoretical cross section for compound nucleus formation,  $\sigma_c$ , for  $\text{Fe}^{56}$  and  $\text{I}^{127}$  calculated for a complex square well with the parameters shown.

the beam energy. The 390-keV line is very weak but is present when the neutron energy is below the threshold of the 435-keV line. A cascade line of 145 keV is reported<sup>34</sup> in coincidence with the 58-keV line. The lines at 145 and 31 keV increased in intensity as the neutron energy decreased and were present below a neutron bombarding energy of 150 keV. This suggests that they arise from capture and may not be lines of  $\text{I}^{127}$  at all. The origin of these lines is not known.<sup>35</sup> It is remarkable that only ground state transitions are observed; if cascade transitions did occur with appreciable intensity (greater than 25% of the ground state transition) they would be apparent in the excitation curves. The accuracy of the  $\text{I}^{127}$  intensity data is not as good as for Fe because the decomposition of the spectra leads to some unavoidable uncertainties.

The interpretation of the excitation curves is very difficult because the assignments of the various states are not known. The ground-state particle configuration is  $(g_{7/2})^2(d_{5/2})$  with an assignment of  $5/2+$ .<sup>30</sup> The beta-decay data<sup>34</sup> do not permit an assignment of the excited states. Excitation curves for a number of assignments of the excited states were calculated for the strong coupling case,  $\zeta=0.2$ . Competition for decay to other excited states as well as the ground state was taken into account in the computation of the excitation

<sup>35</sup> The weighted mean iodine  $K$  x-ray energy is 29 keV so we first interpreted the 31-keV line as the x-ray line from internal conversion. However, the gamma ray source is inside the detector crystal so conversion x-rays could not be observed. Furthermore, the excitation does not follow that of any of the  $\text{I}^{127}$  lines.

functions. The magnitude of the cross section decreases in the following order for the excited state spin assignment:  $7/2$ ,  $5/2$ ,  $3/2$ ,  $9/2$ , and  $1/2$ . In each case the curves for assignments which seem most reasonable are shown, but again the experimental data cannot be used to determine spins. The data of Guernsey<sup>29</sup> show the same general trend for the 62-, 208- and 435-keV excitations in the regions where the data overlap.

If one uses the total inelastic cross section as a lower limit on the cross section for compound nucleus formation, then the data can be used to determine the values of  $\zeta$  one must use. Equation (4) relates this cross section to the transmission coefficients  $T_l$  which are functions of  $\zeta$ . Figure 14 shows the theoretical value of the cross section,  $\sigma_c$ , as a function of neutron energy for  $\text{Fe}^{56}$  and  $\text{I}^{127}$ .  $\text{Fe}^{56}$  is close to a giant  $S$ -wave resonance and  $\text{I}^{127}$  is in a trough between  $P$  and  $S$  maxima. For comparison the values of  $\sigma_{\text{in}}(\text{total})$  for  $\text{I}^{127}$  are plotted at the bottom of Fig. 12. Contributions from only the four levels for which excitation curves are known are included. Table II summarizes the data for  $\text{Mn}^{55}$ ,  $\text{Fe}^{56}$ , and  $\text{I}^{127}$ . The reaction cross section,  $\sigma_r$ , is given by  $\sigma_r = \sigma_{\text{in}} + \sigma_{\text{cap}}$ . The capture cross section,  $\sigma_{\text{cap}}$ , is a small contribution to  $\sigma_r$ . (For  $\text{I}^{127}$ , see curves given in reference 16.) Since  $\sigma_c$  includes all reactions as well as compound elastic scattering, it should always exceed  $\sigma_r$ . The value of  $\sigma_{\text{in}}$  for  $\text{I}^{127}$  may continue to increase as more levels contribute to the inelastic scattering.<sup>36</sup> The theoretical curves for  $\sigma_c$  do not rise rapidly with neutron energy above 1 MeV so these data would support the conclusion that for  $\text{I}^{127}$  at  $E_n=1.2$  MeV the value of  $\zeta=0.2$  gives the best agreement. This conclusion is independent of the model for inelastic scattering.

### Fluorine

The first four excited states of  $\text{F}^{19}$  at 110 and 197 keV at 1.35 and 1.57 MeV have been investigated by neutron scattering, particle reactions, and beta decay.<sup>37</sup> We did not carry out a complete study of  $\text{F}^{19}$ , but Fig. 15 shows the excitation curves obtained. These have not been corrected for the neutron energy spread which is indicated by the triangles. The data up to  $E_n=1.2$  MeV

TABLE II. Comparison of measured reaction cross sections with cross sections for compound nucleus formation.

Element	Neutron energy MeV	$\sigma_c$		$\sigma_r(\text{total})$
		$\zeta=0.04$	$\zeta=0.2$	
Mn	1.2	0.92	1.15	$0.77 \pm 0.15$
Fe	1.2	0.92	1.15	$0.60 \pm 0.08$
	1.8	0.70	1.14	$0.90 \pm 0.12$
I	0.5	0.79	1.59	$0.93 \pm 0.20$
	1.2	1.18	1.63	$1.65 \pm 0.35$

<sup>36</sup> The excitation curves for  $\text{I}^{127}$  should show the effects of competition from higher levels. There was no marked effect noticeable, however Guernsey<sup>29</sup> finds that the excitation of the 62-keV line does decrease above 600 keV.

<sup>37</sup> F. Ajzenberg and T. Lauritsen, *Revs. Modern Phys.* **27**, 77 (1955); C. F. Barnes, *Phys. Rev.* **97**, 1226 (1955).

were taken with a teflon scatterer 1.1 cm thick by 4 cm in diameter. From 1.2 Mev to 1.8 Mev, a right circular cylinder of Teflon 4 cm in diameter by 3.8 cm in length was used. The yields of the 0.110-, 0.197- and 1.37-Mev radiations follow the resonance structure of the total neutron cross section, although some of the detail is lost because of the beam energy spread. No attempt was made to compute cross sections or to match the data obtained with the two scatterers. The threshold for the 1.37-Mev radiation is at  $1.55 \pm 0.02$  Mev indicating that the state at 1.57 Mev decays mainly to the 0.197-Mev state.<sup>38</sup> The resonance structure of the compound state is too complicated to warrant a detailed analysis of the data in terms of single resonances. Also the statistical assumptions of Hauser and Feshbach<sup>6</sup> are probably not valid here, so an interpretation of these data would be very difficult from that viewpoint. High-resolution data might yield more useful information about the levels in  $F^{20}$ .

A search was made in several nuclei for gamma rays from low-lying levels. Levels in  $P^{31}$  at 0.4 and 0.9 Mev<sup>39</sup> have been reported. No excitation was found so we conclude that the cross section must be less than 0.05 b and 0.15 b, respectively for the two lines at a neutron energy of 1.2 Mev. Recently, Olness and Lewis<sup>40</sup> confirmed the absence of low-lying levels by inelastic proton scattering from  $P^{31}$ . The data of Walt<sup>41</sup> indicates a large value for the reaction cross section at 1 Mev in Sr. We found no evidence for inelastic neutron scattering; an upper limit of 0.26 b was placed on this cross section.

#### CONCLUSION

The evidence from excitation curves for  $Mn^{55}$ ,  $Fe^{56}$ , and  $I^{127}$  and the angular distribution of the 850 keV radiation from  $Fe^{56}$  is consistent insofar as it requires a value of the absorption parameter  $\zeta = 0.2$ . This value corresponds to an almost "black" nucleus. In the same energy range elastic neutron scattering data<sup>41,41</sup> suggest the much smaller  $\zeta$  value of 0.03 to 0.05. However, at 4-Mev neutron energy the angular distribution of the elastically scattered neutrons indicates that a value of  $\zeta$  between 0.1 and 0.2 is necessary.<sup>8</sup> The square well model is certainly not correct and a diffuse nuclear boundary should be a better approximation.<sup>42</sup> Oleksa<sup>43</sup>

<sup>38</sup> Day<sup>32</sup> has found gamma rays of 1.24, 1.35, 1.44, and 1.56 Mev with relative intensities of 0.17, 1.00, 0.19, and 0.07, respectively at  $E_n = 2.5$  Mev. We would have missed all but the strongest line in our observations.

<sup>39</sup> P. M. Endt and J. C. Kluyver, *Revs. Modern Phys.* **26**, 95 (1954).

<sup>40</sup> J. W. Olness and H. Lewis, *Phys. Rev.* **99**, 654(A) (1955).

<sup>41</sup> M. Walt and H. H. Barschall, *Phys. Rev.* **93**, 1062 (1954).

<sup>42</sup> Quantitative results on calculations carried out by Porter<sup>4</sup> for the diffuse boundary are not yet available.

<sup>43</sup> S. Oleksa (to be published).

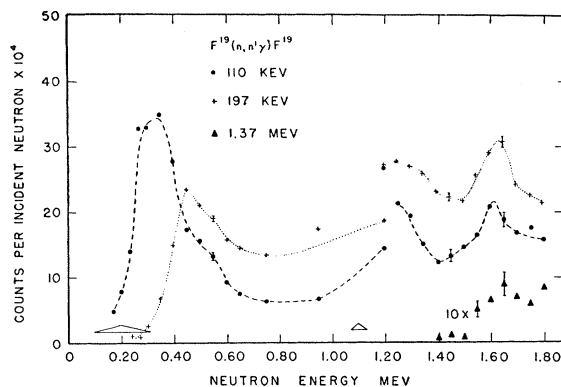


Fig. 15. Excitation curves taken with a teflon sample of the levels at 110 and 119 keV in  $F^{19}$ . The excitation curves are not corrected for neutron energy spread which is indicated by the triangles. It shows the marked effect of resonances which appear also in the total cross section. A third gamma ray of 1.37 Mev is observed above 1.55-Mev neutron energy. The curves above 1.20 Mev were taken with a different sample so yields cannot be compared. All three curves go through a broad resonance peak at 1.6 Mev.

has attempted to fit the Hauser-Feshbach theory to the excitation of the  $13/2+$  level of  $Pb^{207}$ . The fit is very sensitive to the values of  $V_0$  and  $\zeta$ ; however, with  $\zeta$  about 0.03, she was able to obtain a reasonable fit with a rather small change in  $V_0$ . An investigation is being made to determine the contribution to the inelastic scattering from the process of direct excitation through coupling of the incoming neutron to the collective modes of the target nucleus. At present it appears that inelastic scattering data cannot be used to make spin assignments to excited states. A better understanding of the nature of the interactions is needed to permit an interpretation of the data. In certain special cases however the inelastic scattering data provide the most direct measure of the complex part of the interaction potential.

#### ACKNOWLEDGMENTS

We wish to thank Dr. D. Moffatt for considerable aid during the experimental investigations and for the opportunity to discuss the results with him. We also wish to thank R. H. Davis, A. Divatia, and R. Greiner for assistance in the experimental phase of the work. The aid of Dr. R. G. Thomas of the Los Alamos Scientific Laboratory who provided us with the numerical results for the complex square well is gratefully acknowledged.

*Note added in proof.*—Freeman [*Phys. Rev.* **99**, 1446 (1955)] has reported excitation curves for radiations of 0.111, 0.197, 1.24, and 1.37 Mev excited by inelastic neutron scattering in  $F^{19}$ .